



HAL
open science

Biocompatible Magnetic Microspheres for Use in PDT and Hyperthermia

C. B. Vaccari, N. N. P. Cerize, P. C. Morais, Maria-Inês Ré, A. C. Tedesco

► **To cite this version:**

C. B. Vaccari, N. N. P. Cerize, P. C. Morais, Maria-Inês Ré, A. C. Tedesco. Biocompatible Magnetic Microspheres for Use in PDT and Hyperthermia. *Journal of Nanoscience and Nanotechnology*, 2012, 12 (6), pp.5111-5116. 10.1166/jnn.2012.4950 . hal-01688408

HAL Id: hal-01688408

<https://hal.science/hal-01688408>

Submitted on 16 Oct 2020

HAL is a multi-disciplinary open access archive for the deposit and dissemination of scientific research documents, whether they are published or not. The documents may come from teaching and research institutions in France or abroad, or from public or private research centers.

L'archive ouverte pluridisciplinaire **HAL**, est destinée au dépôt et à la diffusion de documents scientifiques de niveau recherche, publiés ou non, émanant des établissements d'enseignement et de recherche français ou étrangers, des laboratoires publics ou privés.

Biocompatible Magnetic Microspheres for Use in PDT and Hyperthermia

C. B. Vaccari¹, N. N. P. Cerize³, P. C. Morais², M. I. Ré^{3,4}, and A. C. Tedesco^{1,*}

¹*Departamento de Química, Centro de Nanotecnologia e Engenharia Tecidual-Lab.de Fotobiologia e Fotomedicina, Faculdade de Filosofia, Ciências e Letras de Ribeirão Preto, Universidade de São Paulo, Ribeirão Preto SP 14040-901, Brazil*

²*Universidade de Brasília, Instituto de Física, Brasília DF 70910-900, Brazil*

³*IPT-Institute of Technological Research of São Paulo State, Centre of Processes and Products Technology, São Paulo SP, Brazil*

⁴*Research Center of Albi on Particulate, Energy and Environment (Centre RAPSODEE), Ecole de Mines Albi, France*

Loaded microspheres with a silicon (IV) phthalocyanine derivative (NzPC) acting as a photosensitizer were prepared from polyhydroxybutyrate-co-valerate (PHBHV) and poly(ε-caprolactone) (PCL) polymers using the emulsification solvent evaporation method (EE). The aim of our study was to prepare two systems of these biodegradable PHBHV/PCL microspheres. The first one containing only photosensitizer previously incorporated in the PHBHV and poly(ε-caprolactone) (PCL) microspheres and the second one with the post magnetization of the DDS with magnetic nanoparticles. Magnetic fluid is successfully used for controlled incorporation of nanosized magnetic particles within the micron-sized template. This is the first time that we could get a successful post incorporation of nanosized magnetic particles in a previously-prepared polymeric template. This procedure opens a great number of possibilities of post-functionalization of polymeric micro or nanoparticles with different bioactive materials. The NzPC release profile of the systems is ideal for PDT, the zeta potential and the size particle are stable upon aging in time. *In vitro* studies were evaluated using gingival fibroblastic cell line. The dark cytotoxicity, the phototoxicity and the AC magnetic field assays of the as-prepared nanomagnetic composite were evaluated and the cellular viability analyzed by the classical test of MTT.

Keywords: Microspheres Biodegradable, Hyperthermia, PDT, Magnetic Nanoparticle, Magnetic Fluid.

1. INTRODUCTION

The interest in nanoscale magnetic drug delivery systems (MDDS) has grown exponentially in the last decade. In principle, there are two systems to be considered here; firstly a more complex material system which pre-encapsulates both the nanosized magnetic particle and the drug within the hosting biodegradable particle,¹ and secondly the drug-dressed magnetic nanoparticle formulated as a biocompatible vehicle.² The development of nanoscale MDDS has demonstrated that both approaches present appropriate stability, higher absorption rates by biological tissues, and excellent target specificity. In addition, microspheres-based MDDS have been associated with controlled release, quantitative transfer and

high pharmacodynamic activity inside the organism, as expected from the new generation of drugs developed to target cancer and other skin diseases.³ Likewise, biocompatible magnetic fluids (BMF) have been pointed out as a very promising nanosized-based magnetic material applicable to tumor therapy. The therapeutic approach has essentially focused on local hyperthermia of biological tissues, induced by the application of low-frequency, low-amplitude AC external magnetic fields.⁴

This study, however, reports on the first successful post-incorporation of nanosized magnetic particles within a previously drug-loaded polymeric template. This approach opens up a great number of new possibilities for post-functionalization of polymeric micro- or nano-particulated templates encapsulating different bioactive materials. Polymer blends containing biodegradable components are of great interest due to the possibility of tailoring their

* Author to whom correspondence should be addressed.

physico-chemical properties and responses while in biological medium. These materials have attracted quite a lot of attention, especially in relation to their application for biomedical use.^{5,6} The use of biodegradable polymeric microspheres as templates in MDDS for *in vitro* studies allows the investigation of the influence of physical, chemical, photobiological and photochemical factors controlling the uptake of nanosized magnetic particles and photosensitizers by tissues. In addition, the *in vitro* assays also provide insights into the mechanisms involved in both magnetohyperthermia (MHT) and photodynamic therapy (PDT) approaches and the subsequent thermal and photoinduced necrosis or apoptosis in neoplastic tissues. In this study we report on the production and the use of biodegradable polyhydroxybutyrate-co-valerate/polycaprolactone (PHBHV/PCL) microspheres,^{7,8} incorporating a silicon (IV) phthalocyanine derivative (NzPC) as the photosensitizer agent and nanosized maghemite particles. Actually, the citrate-coated maghemite nanoparticles were successfully post-incorporated within the previously NzPC-loaded PHBHV/PCL microsphere. Gingival fibroblast was used as a classical biological model to evaluate the thermal and the photobiological activity of the as-produced MDDS, including the synergic effects of MHT and PDT.

2. MATERIALS AND METHODS

2.1. Preparation of NzPC-Loaded Microspheres and Post-Incorporation of Nanosized Maghemite

In a preliminary step the biocompatible/biodegradable NzPC-loaded PHBHV/PCL microsphere (NzPC-PHBHV/PCL μ s) was produced using the emulsification-solvent evaporation (EE) method, as described in the literature.⁹ The NzPC used was the silicon tribenzoporphyrinato with two *n*-dimethylaminoethanoyl as axial groups on silicon. The developed magnetic nanocomposite (Nmag-NzPC-PHBHV/PCL μ s) post-incorporated citrate-coated nanosized maghemite (γ -Fe₂O₃) particles within the previously prepared NzPC-PHBHV/PCL μ s hosting template. The citrate-functionalized maghemite nanoparticle was formulated as a BMF sample according to the literature¹⁰ and used in a subsequent step to associate with the NzPC-PHBHV/PCL μ s under agitation at 37 °C, for 1 h. The average core maghemite diameter, as obtained from transmission electron microscopy, was 7.7 nm. While suspended within the BMF the citrate-coated maghemite particles presented an average hydrodynamic size of 62 nm and zeta potential of -52.1 mV. Incorporation of the magnetic phase within the polymeric template employed a device especially designed for keeping the sterilization process; the same device used to prepare the hosting template. The used protocol allowed successful incorporation of the nanosized magnetic particles within NzPC-PHBHV/PCL μ s. Based on the spectroscopy properties of the NzPC dye used and the amount of material recovered after

isolation of the magnetic NzPC-PHBHV/PCL μ s, from the medium, we evaluated that an average of 93% of NzPC-loading was achieved. The same range as the result obtained by direct determination of the iron inside the final MDDS (Nmag-NzPC-PHBHV/PCL μ s). We also found that the new material presented a good response to the AC applied magnetic field while being used for MHT. Figure 1 shows typical scanning electron microscopy micrographs of samples NzPC-PHBHV/PCL μ s (Fig. 1(a)) and Nmag-NzPC-PHBHV/PCL μ s (Fig. 1(b)).

2.2. Evaluation of Maghemite Incorporation

After the step of maghemite encapsulation, the produced Nmag-NzPC-PHBHV/PCL μ s MDDS was washed with ultrapure water, centrifuged, and lyophilized. In order to quantify free Fe³⁺ in solution the supernatant (washed water) was collected and oxidized using HCl/HNO₃ (3:1, v/v). The oxidized solution was complexed with

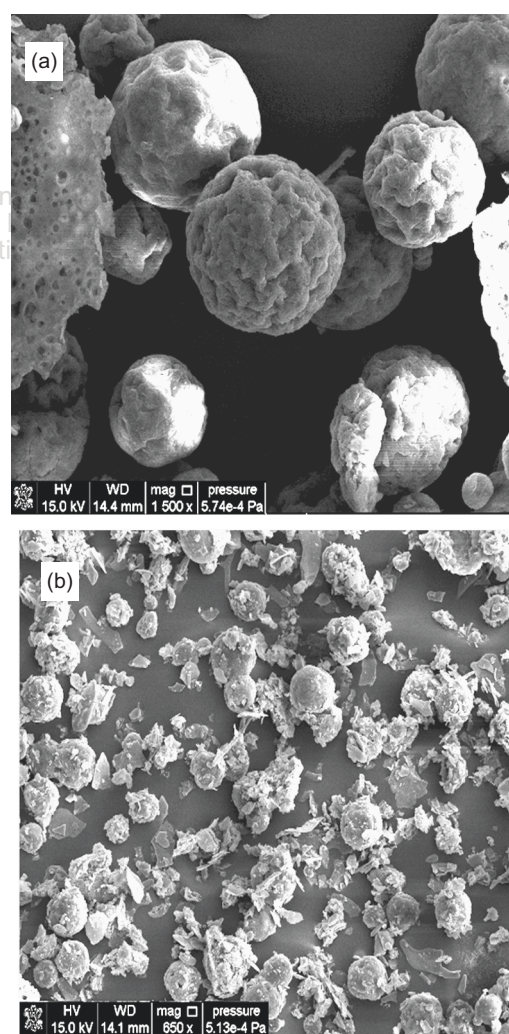


Fig. 1. Scanning electron microscopy of samples (a) NzPC-PHBHV/PCL μ s and (b) Nmag-NzPC-PHBHV/PCL μ s.

Tiron[®], thus producing a red color for spectrophotometry evaluation at 480 nm.¹¹ It was found that the yield of incorporation of maghemite within the polymeric template reached about 95%.

2.3. Zeta Potential and Particle Size

Samples NzPC-PHBHV/PCL μ s and Nmag-NzPC-PHBHV/PCL μ s were evaluated in regard to Zeta potential and hydrodynamic diameter. The data were recorded as a function of time up to 60 days using the Malvern Zetasizer Nanoseries (Malvern Instruments, UK).

2.4. Evaluation of NzPC Bioavailability for Release Profile

The bioavailability of the photosensitizer (NzPC) was evaluated for samples NzPC-PHBHV/PCL μ s and Nmag-NzPC-PHBHV/PCL μ s, after their incubation with human plasma (HP) extracted from healthy patients. The HP was provided by the Hemocentre of the University of São Paulo (Ribeirão Preto, Brazil) and approved by the ethics committee in human research. Quantification of the NzPC released from the polymeric template due to degradation of the HP-incubated samples was performed by spectrofluorometry while exciting the samples with the 613 nm wavelength light, at 37 °C, and recording the emission at 678 nm. For measurements, samples were collected in quartz cuvettes with 1 cm optical path length. Typically, 3.0 μ mol.L⁻¹ of NzPC in 2 mL of HP was used for measurements. The measurements were carried out using the FluoroLog-3 system (SPEX Jobin Yvon, France) equipped with a temperature control unit and magnetic agitation.

2.5. Cell Culturing

The cell line used in this study was the classical gingival fibroblastic (GF) supplied by the Faculty of Dentistry of the University of São Paulo (Ribeirão Preto, Brazil). The GF was collected from healthy patients and the protocol approved by the ethics committee in human research. Monolayer cultures were grown in Dupleco Eagle's Minimum Essential Medium (DMEM) with 10% fetal bovine serum (Gibco), 1% L-glutamine, and 1% penicillin–streptomycin (Gibco). Cells were used in the logarithmic phase of growth and maintained at 37 °C in humidified 5% CO₂ and 95% air.

2.6. Cytotoxicity and Photocytotoxicity

The methodology used to evaluate the cytotoxicity was the classical MTT assay.¹² The tetrazolium salt [3-(4,5-dimethylthiazol-2-yl)-2,5-diphenyl tetrazolium bromide] (MTT) produced the highly colored formazan dye upon NADH reduction, which reflects a living cellular dehydrogenase.

To investigate the cell toxicity and phototoxicity suspensions containing 5×10^3 GF cells in 500 μ L of medium were inoculated into each well in a 24-well microplate. After culturing in a CO₂ incubator for 24 h monolayer cultures of GF were treated with samples NzPC-PHBHV/PCL μ s and Nmag-NzPC-PHBHV/PCL μ s.¹³ After 3 h incubation in dark condition the cells were washed and the volume was completed by adding 500 μ L DMEM in each well, for 24 h. The 1.0 mg.mL⁻¹ MTT solution (80 μ L per well) was added to 420 μ L per well of DMEM and added to the cells on all 24-well plates, then followed by incubation for 4 h, at 37 °C. The crystals which formed due to the interaction between the mitochondrial dehydrogenases and the MTT reagent were dissolved with 2-propanol. The samples were shaken until complete dissolution of the formed product. After completing the color reaction the absorbance of each well at 560 and 690 nm was measured with Safire II (TECAN). The percentage of cell vitality was calculated with respect to the control cells non-incubated with the polymeric-based structures.

The phototoxicity tests used the visible light set at 675 nm provided by a diode laser Eagle (Quantum Tech, Brazil). The applied light dosage was first evaluated with respect to the biological response. The cells were incubated with NzPC-PHBHV/PCL μ s for 3 h, washed with PBS and then laser irradiated with 1.0, 5.0 and 10.0 J.cm⁻². The laser irradiation at 10.0 J.cm⁻² showed the best biological response.¹

2.7. Evaluation of AC Magnetic Field Application

In the combined MHT/PDT experiment, using laser irradiation following AC magnetic field application, the cells were incubated with the Nmag-NzPC-PHBHV/PCL μ s sample for 3 h. After 3 h incubation the cells were washed with PBS and fresh DMEM was added. Then, laser irradiation at 10.0 J.cm⁻² following exposure to the AC magnetic field (1 MHz at 40 Oe field amplitude) was applied 3 times, 10 min. duration for each application, every hour.³

2.8. Statistical Analysis

All experiments were done in duplicate and the statistical significance (*p*-value) was determined using Student's test (*p*-values < 0.05 mean the results are significant).

3. RESULTS AND DISCUSSION

3.1. Morphology of the Polymeric Microspheres from Scanning Electron Microscopy

The scanning electron microscopy micrograph presented in Figure 1(a) clearly shows the porous nature of the hosting polymeric template. The porous structure of the polymeric template holds even after incorporation of the magnetic nanoparticles (Fig. 1(b)). This observation explains the

high yield of nanosized maghemite incorporation while the hosting NzPC-PHBHV/PCL μ s is mixed with the BMF sample to produce sample Nmag-NzPC-PHBHV/PCL μ s. Due to the spherical symmetry of the hosting polymeric material and the diffusion-related process of maghemite nanoparticles into the template the concentration of the incorporated nanosized magnetic particles is expected to increase from the center up to the surface of the polymeric microsphere, as already described in the literature.¹⁴ As discussed later on in this paper this finding may have a strong effect upon the negative charge held by samples NzPC-PHBHV/PCL μ s and Nmag-NzPC-PHBHV/PCL μ s, as obtained by zeta potential evaluation.

3.2. Zeta Potential and Particle Size

The zeta potential data and the hydrodynamic particle size evaluation support the observed physico-chemical stability and reveal the size homogeneity of the as-prepared micron-sized polymeric particles (see Table I). No appreciable variation on the average values of zeta potential and hydrodynamic particle size characteristics was observed up to 60 days of samples evaluations. As shown in Table I the nanomagnetic-loaded microspheres (sample Nmag-NzPC-PHBHV/PCL μ s) presented negative zeta potential values much higher than the nanomagnetic-unloaded microspheres (sample NzPC-PHBHV/PCL μ s), which is more likely related to the negative charge of the citrate groups attached to the nanosized maghemite surface. This picture is consistent with the high colloidal stability of the BMF sample upon dispersion and the high negative value of the zeta potential.¹⁵ Actually, this finding is also consistent with the picture of a higher concentration of the citrate-functionalized maghemite particles near the polymeric microsphere surface. The negatively-charged carboxylate groups respond to the enhancement of the zeta potential of the polymeric microsphere holding the surface-functionalized nanoparticles. Nevertheless, though different in magnitude, the negative charge associated with both samples (NzPC-PHBHV/PCL μ s and Nmag-NzPC-PHBHV/PCL μ s) provide them with the observed stability upon aging in the time window of our observation (60 days). In agreement with the higher zeta potential sample Nmag-NzPC-PHBHV/PCL μ s also presented larger hydrodynamic average size, as the effective thickness of

Table I. Average values of hydrodynamic size, diameter dispersion and zeta potential of samples NzPC-PHBHV/PCL μ s and Nmag-NzPC-PHBHV/PCL μ s.

Sample	Hydrodynamic diameter (μ m)	Size dispersion (μ m)	Zeta potential (mV)
NzPC-PHBHV/PCL μ s	39.04 \pm 0.31	0.32 \pm 0.04	-3.6 \pm 0.4
Nmag-NzPC-PHBHV/PCL μ s	58.61 \pm 0.28	0.22 \pm 0.05	-12.6 \pm 0.6

the adsorbed solvation layer around the polymeric microsphere extends longer within the aqueous medium.

3.3. Release Profile of NzPC for the Two Material Systems

The drug (NzPC) release profile seems to be equally influenced by the distribution of the incorporated nanosized maghemite particles within the hosting polymeric template while the samples (NzPC-PHBHV/PCL μ s and Nmag-NzPC-PHBHV/PCL μ s) are incubated with HP for bioavailability evaluation.

Figure 2 shows the NzPC release profile of samples NzPC-PHBHV/PCL μ s (Fig. 2(a)) and Nmag-NzPC-PHBHV/PCL μ s (Fig. 2(b)), revealing a peak of NzPC release at 24 and 12 hours after incubation with HP, respectively. Nevertheless, as observed in Figures 2(a and b), the maximum of the fluorescence emission is about the same for both evaluated samples. This observation is a strong

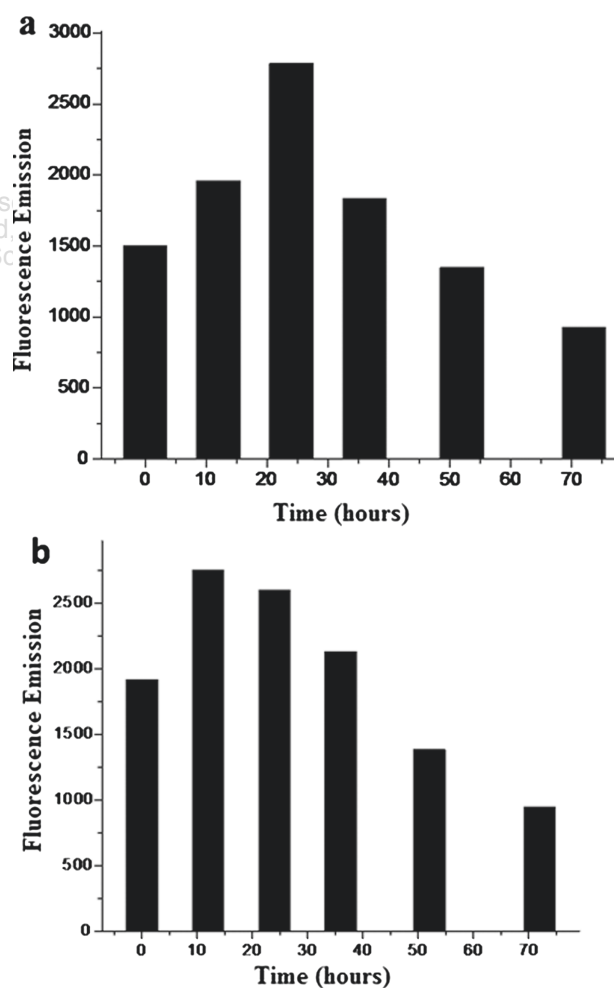


Fig. 2. Time dependence of the fluorescence emission intensity for excitation at 613 nm wavelength during the degradation assays of the loaded microspheres. (a) sample NzPC-PHBHV/PCL μ s and (b) sample Nmag-NzPC-PHBHV/PCL μ s.

argument for the assumption that the drug release mechanism is the same for both samples, more likely dominated by diffusion of NzPC out of the porous polymeric microspheres. The observed peak-shift (from 24 down to 12 hours) indicates the enhancement of the NzPC diffusion coefficient within sample Nmag-NzPC-PHBHV/PCL μ s in comparison with sample NzPC-PHBHV/PCL μ s. We claim that incorporation of the surface-functionalized maghemite nanoparticles within the polymeric template is responsible for the enhancement of the NzPC diffusion coefficient. The drug release profile shown in Figure 2(b) is ideal for PDT, showing a burst on the initial release and sustained after time.

3.4. *In Vitro* Assay, Cellular Viability

Figure 3 summarizes the results of the *in vitro* cytotoxicity assays, revealing well accepted values as a basal level for the used cell line (8%), which suggests no cytotoxicity of the employed material system (sample Nmag-NzPC-PHBHV/PCL μ s).¹⁶ The data of dark toxicity is reduced by approximately 10% when compared with other DDS used for PDT.¹⁷ The phototoxicity assay alone (dose light irradiation at 10.0 J.cm⁻²) using sample NzPC-PHBHV/PCL μ s showed that the system presented a very good response to the light treatment, a factor that reinforces the use of the system in studies as a promising DDS with expected good outcomes for this therapy. For the AC magnetic field assay the employed MDDS (sample Nmag-NzPC-PHBHV/PCL μ s) presented a good response. This observation can be attributed to the efficiency of the local heating caused by the hyperthermia process. However, the combined toxicity study comprising the laser irradiation plus the application of the AC magnetic field confirmed the presence of a synergic effect¹⁸ with a clear enhanced response as far as the cell viability is concerned (15.2%), as shown in Figure 3. This data confirms that the amount of dye released in the biological medium was accelerated,

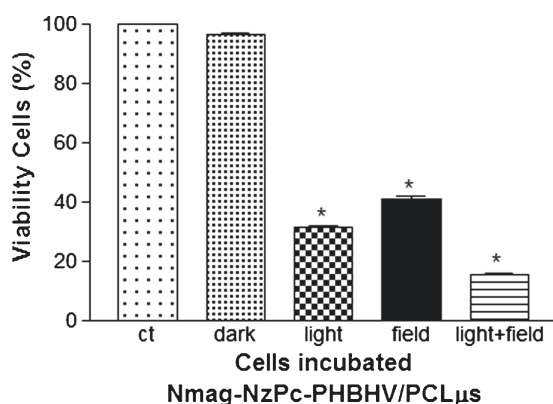


Fig. 3. Evaluation of the cellular viability using fibroblast gingival cells incubated with sample Nmag-NzPC-PHBHV/PCL μ s; in dark condition, under laser light (10 J.cm⁻²), under AC magnetic field, and in the presence of both laser light and AC magnetic field.

reaching a higher drug level in the target tissue after 12 h, in agreement with the results obtained in the biodegradation studies. This finding represents an extremely important step for planning *in vivo* experiments using healthy and tumor-induced animals, before phase-I in humans can be put forward.

4. CONCLUSIONS

The present study allowed evaluation of the biological effects due to the use of the produced and characterized polymeric-based magnetic nanocomposite. Post-incorporation of maghemite nanoparticles (via a biocompatible magnetic fluid) in a previously-prepared polymeric template of PHBV/PCL μ s was a success; the data of quantification showed values of 95% of magnetic incorporation. The presence of magnetic particles within the polymeric system brought larger stability, enhancing the zeta potential due to the increase of the negative charge, favoring their stability upon dispersion. In addition, the incorporated magnetic particle increased the diffusion of NzPC out of the porous polymeric microspheres, with a burst of the initial drug release and sustainability after the time ideal for PDT. Our evaluation was also accomplished by analyzing the cellular viability under photoactivation combined or not with the hyperthermia treatment, using a well know cellular system as the biological model. Our data indicate that the MDDS system investigated here is biocompatible and can be used as material basis for biological applications. The sample works efficiently under light and AC magnetic field for cell death, opening up the possibility of delivering other actives molecules for cancer treatment.

Acknowledgments: The authors acknowledge the financial support of the Brazilian agency FAPESP (process #06/57129-1, 07/55319-0, 08/53719-4), CNPq #573880/2008-5 (INCT) and the help of Dr. Fernando Lucas Primo and Dr. Andreza Ribeiro Simioni of the FFCLRP-USP in the experiments.

References and Notes

1. A. R. Simioni, C. Vaccari, and M. I. Re, *J. Mater. Sci.* 43, 580 (2008).
2. D. M. Oliveira, P. P. Macaroff, K. F. Ribeiro, Z. G. M. Lacava, R. B. Azevedo, and E. C. D. Lima et al., *J. Magn. Magn. Mater.* 289, 476 (2005).
3. D. M. Oliveira, Estudos Sinérgicos de fármacos fotossensibilizadores utilizados na Terapia Fotodinâmica e fluidos magnéticos utilizados em Hipertermia celular. Faculdade de Filosofia, Ciências e Letras de Ribeirão Preto-USP (2006).
4. M. H. A. Guedes, N. Sadeghiani, D. L. G. Peixoto, J. P. Coelho, L. S. Barbosa, and R. B. Azevedo et al., *J. Magn. Magn. Mater.* 293, 283 (2005).
5. A. G. A. Coombes, P. D. Scholes, M. C. Davies, L. Illum, and S. S. Davis, *Biomaterials* 15, 673 (1994).

6. S. Kalimoultou, M. Skiba, P. Bon, P. Dechelotte, P. Arnaud, and M. Lahiani-Skiba, [*Journal of Nanoscience and Nanotechnology* 9, 150 \(2009\)](#).
7. M. Avella, E. Martuscelli, and M. Raimo, [*J. Mater. Sci.* 35, 523 \(2000\)](#).
8. J. F. W. Nijsen, M. J. van Steenbergern, H. Kooijman, H. Talsma, L. M. J. Kroon-Batenburg, and M. van de Weert et al., [*Biomaterials* 22, 3073 \(2001\)](#).
9. F. S. Poletto, E. Jager, M. I. Re, S. S. Guterres, and A. R. Pohlmann, [*Int. J. Pharm.* 345, 70 \(2007\)](#).
10. P. C. Morais, R. L. Santos, A. C. M. Pimenta, R. B. Azevedo, and E. C. D. Lima, [*Thin Solid Films* 515, 266 \(2006\)](#).
11. S. E. Khalafalla and G. W. Reimers, [*Ieee Transactions on Magnetics* 16, 178 \(1980\)](#).
12. F. Denizot and R. Lang, [*Journal of Immunological Methods* 89, 271 \(1986\)](#).
13. P. A. Barbugli, [*Journal of Nanoscience and Nanotechnology* 10, 569 \(2010\)](#).
14. P. C. Morais, R. B. Azevedo, L. P. Silva, Z. G. M. Lacava, F. P. L. Filho, and A. P. C. Lemos et al., [*Physica Status Solidi A-Applied Research* 201, 898 \(2004\)](#).
15. R. Wongsagonsup, S. Shobsngob, B. Oonkhanond, and S. Varavinita [*Starch-Starke* 57, 25 \(2005\)](#).
16. S. J. H. Soenen, A. R. Brisson, and M. De Cuyper, [*Biomaterials* 30, 3691 \(2009\)](#).
17. D. M. Oliveira, Z. G. M. Lacava, E. C. D. Lima, P. C. Morais, and A. C. Tedesco, [*Journal of Nanoscience and Nanotechnology* 6, 2432 \(2006\)](#).
18. A. R. Simioni, F. L. Primo, M. M. A. Rodrigues, Z. G. M. Lacava, P. C. Morais, and A. C. Tedesco, [*Ieee Transactions on Magnetics* 43, 2459 \(2007\)](#).